Pressure Distribution in a Layered Reservoir with Lateral Wells

E. S. Adewole, B. M. Rai and T. O. K. Audu
Department Of Petroleum Engineering
University of Benin, Benin City, Nigeria.

Abstract.

The production of oil and gas from a layered reservoir using lateral wells at economic rates has been a major problem to both the reservoir and production engineers. The problem manifests in such wells when they cannot deliver fluid at the desired rates and volumes, good enough to justify the level of investment (measured by discovery, drilling and completion efforts.) This is often traceable to lack of good understanding of fluid dynamics in layered reservoirs when they are drilled with lateral drainholes. In this paper, mathematical models are constructed to study pressure distribution in a layered reservoir, with and without crossflow, containing lateral wells. The pressure distributions are utilized to investigate the wellbore, reservoir layers and layers fluid conditions best suited for optimum oil recovery.

pp 135 - 146

1.0 Introduction

When a reservoir is layered then the reservoir has more than one clearly identifiable permeability distribution and an interface. If the layers are in communication (cross flow), fluid will flow into the layer of larger permeability, and therefore, the layer fluids can e produced through one well. On the other hand, if the layers are not in communication (no cross flow) then the layers fluids are either commingled or produced separately.

In this paper, the candidacy of lateral wells, as oil producers or fluid injectors in a layered reservoir, is investigated in terms of well bore pressure distribution.

Pressure distribution studies in layered reservoirs, for now, are more popular fro vertical wells [1], [2]. But [3] and [4] proposed theoretical studies of fluid flow in multi-layered reservoirs involving horizontal wells basically to permit identification of flow periods, reservoir layers boundaries and well bore conditions. These authors modelled only one horizontal well in a stratified reservoir as a case of extended single layer reservoir with crossflow. Recently [5] and [6] utilized pressure distribution in a layered reservoir to study the effect of length on wellbore productivities. Test analysis of pressure from layered reservoirs was discussed by [6]. We intend, in this paper, to extend the frontiers of [5] and [6]. Green's and source functions developed in [7] and [9] will be utilized to derive all pressure distribution expressions.

2.0 Layered Reservoir and Mathematical Models Descriptions

The stratified model shown in Figure 1 consists of two drainholes. There are two clearly identifiable layers. Between the identified layers, here is an interface, which may be permeable or impermeable. Each layer contains fluid of small and constant compressibility but the layers do not necessarily the same viscosity. The wells are assumed to be parallel to pair of top and bottom no-flow boundaries and each is located in a semi-infinite rectangular drainage region. The wells produce or receive fluid at a constant rate across the sand face of each wellbore. Each layer's pressure before production, injection or buildup is p_j. We wish to derive a relationship between p_j, reservoirs layers, layers' fluids, and wellbore properties with time, to gain an insight into the fluid dynamics in he layered reservoir subject to a pressure transient. The wells have radii r_{wj}, along the y and z axes, and lengths L_j, along the x-axis. The widths of the wells (along the y-axis) are $y_{wj} = 0$ to $y_{wj} = \infty$ in width; that is, each layer is semi-infinite in dimension. Each well is z_{wj} away from its no-flow vertical boundary and each layer is h_{wj} thick. Therefore, the op of the bottom layer is the location of the interface. The reservoir layers are considered to be largely anisotropic. and all permeabilities are considered to be independent of pressure. However, production or injection pressures are assumed to be above

bubble point of oil. As there are no external recharging boundaries either at the top or bottom of reservoir, the energy for fluid flow is derived strictly from the dissolved gas in the oil or from fluid injection pressure. Skin effects and wellbore storage problems are considered negligible.

The wells therefore, experience source strengths, along the x-axis, from an infinite slab in an infinite reservoir along y-axis. The z-axis sources are, however, dependent on whether the interface is permeable (crossflow) or not (no crossflow.) For no crossflow, the source strengths from the z-axes are originating from infinite plane sources in infinite slab reservoirs.

For crossflow layers, the z-axis represents a mixed boundary situation as shown in Figure 2. Here the interface is assumed to be similar to a partially-constant-pressure boundary. Therefore, if the individual layers are considered separately, the top layer has a partially recharging boundary at the top, similar to a gas cap. Therefore, the z-axis source functions for each layer must contain a weighting factor which accounts for his dual-natured boundary effects at the interface. Considering the above description, the following source functions can be written as discussed in [7], [9] and [16].

x-axis

$$s\left(x_{Dj},t_{Dj}\right)=\frac{1}{4}\left[erf\left(\frac{1+x_{Dj}}{2\sqrt{t_{Dj}}}\right)\right]+erf\left(\frac{1-x_{Dj}}{2\sqrt{t_{Dj}}}\right) \tag{2.1}$$

y-axis

$$s\left(y_{Dj},t_{Dj}\right)=\frac{1}{2\sqrt{\pi t_{Dj}}}e^{-\frac{\left(y_{Dj}-y_{wDj}\right)^2}{4t_{Dj}}} \tag{2.2}$$

z-axis

(i) Crossflow

$$s\left(z_{Di},t_{Di}\right)=\frac{E_i}{h_{Di}}\sum_{n=1}^{\infty}\exp\left(-\frac{(2n+1)^2\pi^2 t_{Di}}{4h_{Di}^2}\right)\cos\frac{(2n+1)\pi z_{Di}}{h_{Di}}\cos\frac{(2n+1)\pi z_{wDi}}{h_{Di}} \tag{2.3a}$$

$$s\left(z_{Di+1},t_{Di+1}\right)=\frac{E_{i+1}}{h_{Di+1}}\sum_{n=1}^{\infty}\exp\left(-\frac{(2n-1)^2\pi^2 t_{Di+1}}{4h_{Di+1}^2}\right)\sin\frac{(2n-1)\pi z_{Di+1}}{2h_{Di+1}}\sin\frac{(2n-1)\pi z_{wDi+1}}{2h_{Di+1}} \tag{2.3b}$$

where E_j is the desired weighting factor. j = layer i or $i+1$.

(ii) No Crossflow

$$s\left(z_{Dj},t_{Dj}\right)=\frac{1}{h_{Dj}}\left[1+2\sum_{n=1}^{\infty}\exp\left(-\frac{n^2\pi^2 t_{Dj}}{4h_{Dj}^2}\right)\cos\frac{n\pi z_{Dj}}{h_{Dj}}\cos\frac{n\pi z_{wDj}}{h_{Dj}}\right] \tag{2.4}$$

It should be noted, however, that for the z-axis, like other axes, no matter the nature of he layers boundaries, an every early flow time (infinite-acting flow time) the generally applicable source function is an infinite plane source in an infinite reservoir given as

$$s\left(z_{Dj},t_{Dj}\right)=\frac{1}{2\sqrt{\pi t_{Dj}}}e^{-\frac{\left(z_{Dj}-z_{wDj}\right)^2}{4t_{Dj}}} \tag{2.5}$$

The dimensionless parameters used are based on wellbore half-length as follows:

$$(1)\qquad m_D=\frac{2m}{L}\sqrt{\frac{k}{k_m}}\qquad \text{where } m=x,y,z \tag{2.6}$$

$$(2)\qquad t_D=\frac{4kt}{\phi\mu c_t L^2} \tag{2.7}$$

$$(3)\qquad L_D=\frac{L}{2h}\sqrt{\frac{k}{k_x}} \tag{2.8}$$

$$h_D = \frac{2h}{L}\sqrt{\frac{k}{k_z}} \tag{2.9}$$

(4)

$$p_{Dj} = \frac{p_j - p(x,y,z,t)}{\Delta_{pj}} \tag{2.10}$$

(5)

With these source functions the dimensionless pressure for each layer is therefore obtained for 3D flow the Newman's product method as

$$p_{Dj}\left(x_D, y_D, z_D, t_{Dj}\right) = 2\pi h_{Dj}\int_0^{t_D} s\left(x_{Dj},\tau\right)s\left(y_{Dj},\tau\right)s\left(z_{Dj},\tau\right)d\tau \tag{2.11}$$

for a constant production or injection rate. To correct for differences in flow times in the two layers as a result of possible differences in flow and layers properties, a common time frame is established by the following definition

$$t_{Di+1} = \beta t_{Di} = \beta t_D \tag{2.12}$$

Therefore,

$$\beta = \frac{\phi_i c_{ti}\mu_i L_i^2 k_{i+1}}{\phi_{i+1}c_{ti+1}\mu_{i+1}L_{i+1}^2 k_{i+1}} \tag{2.13}$$

3.0 Individual Layer Dimensionless Pressure Expressions

3.1 Crossflow Interface

The layers dimensionless pressure expressions are derived according to equation (2.11) as follows:

3.1.1 Layer *i* (Bottom Layer)

$$p_{Di}\left(x_D, y_D, z_D, t_D\right) = \frac{E_i\sqrt{\pi^t}}{2}\int_0^D\left[erf\left(\frac{1+x_D}{2\sqrt{\tau}}\right) + erf\left(\frac{1-x_D}{2\sqrt{\tau}}\right)\right]\frac{e^{-\frac{\left(y_D - y_{wD}\right)^2}{4\tau}}}{\sqrt{\tau}}\sum_{n=1}^{\infty}\exp\left(-\frac{(2n+1)^2}{4h_D^2}\pi^2\tau\right)\cos(2n+1)\pi\frac{z_D}{h_D}\cos(2n+1)\pi\frac{z_{wD}}{h_D}d\tau \tag{3.1}$$

3.1.2 Layer *i* + 1 (Upper Layer)

$$p_{Di+1}\left(x_D, y_D, z_D, t_D\right) = \frac{E_i\sqrt{\pi\beta}}{2}\int_0^{t_D}\left[erf\left(\frac{1+x_D}{2\sqrt{\beta\tau}}\right) + erf\left(\frac{1-x_D}{2\sqrt{\beta\tau}}\right)\right]\frac{e^{-\frac{\left(y_D - y_{wD}\right)^2}{4\tau}}}{\sqrt{\tau}}\sum_{n=1}^{\infty}\exp\left(-\frac{(2n-1)^2}{4h_D^2}\pi^2\beta\tau\right)\sin\tfrac{1}{2}(2n-1)\pi\frac{z_D}{h_D}\sin\left(\frac{2n-1}{2}\right)\pi\frac{z_{wD}}{h_D}d\tau \tag{3.2}$$

Application of the following interface conditions include

(a) pressure equilibrium

$$p_{Di}\left(x_D, y_D, z_D = h_{Di}, t_D\right) = p_{Di+1}\left(x_D, y_D, z_D = h_{Di}, t_D\right) \tag{3.3a}$$

and

(b) equal flow velocities, from Darcy's law

$$\frac{\partial p_{Di}\left(x_D, y_D, z_D = h_{Di}, t_D\right)}{\partial z_D} = -M \frac{\partial p_{Di}\left(x_D, y_D, z_D = h_{Di}, t_D\right)}{\partial z_D} \tag{3.3b}$$

to equations (3.1) and (3.2) yields an eigen value, M, through a zero determinant as

$$M = \frac{I_1 \cdot I_{22}}{I_2 \cdot I_{11}} \tag{3.4}$$

The eigen value, which is the mobility ratio, prescribes the stability condition for fluid displacement through the layers. Solving equations (3.1) and (3.2) using initial and boundary (no-flow) conditions stated respectively as

$p_{Dj}\left(x_D, y_D, z_D, t_D\right) = 0$ and $\frac{\partial p_{Dj}\left(x_D, y_D, z_D = h_D \text{ and } z_D = 0, t_D\right)}{\partial z_D} = 0$, we have that $E_i = E_{i+1}$. At the wellbore, equation (2.10) gives unit dimensionless pressure drop in each layer at $t_{iD} \succ 0$. Therefore, representing equation (2.10) in form of Fourier series we have, for the wellbore

$$\sum_{n=1}^{\infty} p_{wDj}\left(x_D, y_{wD}, z_{wD}, t_{Dj}\right) = 1 \tag{3.5}$$

Using equations (3.1) and (3.2) equation (3.5) is solved to yield [8]

$$E_j = \frac{2}{\sqrt{\pi}} \left[\frac{\int_{z_{wDi}}^{h_{Di}} I_{11} dz_D + \int_{h_{Di}}^{h_D} I_{22} dz_D}{\int_{z_{wDi}}^{h_{Di}} I_{11}^2 dz_D + \int_{h_{Di}}^{h_D} I_{22}^2 dz_D} \right] \tag{3.6}$$

The expression for E in equation (3.6) is imposed on equations (3.1) and (3.2) to duplicate he actual effects of the interface on the pressure distribution. In equation (3.6)

$$I_1 = \frac{1}{h_{Di}} \int_0^{t_D} \left[erf\left(\frac{1+x_{Di}}{2\sqrt{\tau}}\right) + erf\left(\frac{1-x_{Di}}{2\sqrt{\tau}}\right) \right] \frac{e^{-\frac{\left(y_{Di} - y_{wDi}\right)^2}{4\tau}}}{\sqrt{\tau}} \sum_{n=1}^{\infty} (2n+1)\pi \exp\left(-\frac{(2n+1)^2}{4h_{Di}^2} \pi^2 \tau \right) \cos(2n$$

$$+1)\pi \frac{z_{wDi}}{h_{Di}} \sin(2n+1)\pi \frac{z_{Di}}{h_{Di}} d\tau \tag{3.7}$$

$$I_2 = \frac{\sqrt{\beta}}{h_{Di+1}} \int_0^{t_D} \left[erf\left(\frac{1+x_{Di+1}}{2\sqrt{\beta\tau}}\right) + erf\left(\frac{1-x_{Di+1}}{2\sqrt{\tau}\beta}\right) \right] \frac{e^{-\frac{\left(y_{Di+1} - y_{wDi+1}\right)^2}{4\beta\tau}}}{\sqrt{\tau}}$$

$$\sum_{n=1}^{\infty} \frac{(2n-1)}{2} \pi \exp\left(-\frac{(2n-1)^2}{4h_{Di+1}^2} \pi^2 \beta\tau \right) \cos\left(\frac{2n-1}{2}\right) \pi \frac{z_{Di+1}}{h_{Di+1}} \sin\left(\frac{2n-1}{2}\right) \pi \frac{z_{wDi+1}}{h_{Di+1}} d\tau \tag{3.8}$$

$$I_{11} = \int_0^{t_D} \left[erf\left(\frac{1+x_{Di}}{2\sqrt{\tau}}\right) + erf\left(\frac{1-x_{Di}}{2\sqrt{\tau}}\right) \right] \frac{e^{-\frac{\left(y_{Di} - y_{wDi}\right)^2}{4\tau}}}{\sqrt{\tau}} \sum_{n=1}^{\infty} \exp\left(-\frac{(2n+1)^2}{4h_{Di}^2} \pi^2 \tau \right) \cos(2n$$

$$+1)\pi \frac{z_{wDi}}{h_{Di}} \cos(2n+1)\pi \frac{z_{Di}}{h_{Di}} d\tau \tag{3.9}$$

$$I_{22} = \sqrt{\beta}\int_0^{t_D}\left[erf\left(\frac{1+x_{Di+1}}{2\sqrt{\beta\tau}}\right)+erf\left(\frac{1-x_{Di+1}}{2\sqrt{\tau}\beta}\right)\right]\frac{e^{-\frac{\left(y_{Di+1}-y_{wDi+1}\right)^2}{4\beta\tau}}}{\sqrt{\tau}}$$

$$\sum_{n=1}^{\infty}\frac{(2n-1)}{2}\pi\exp\left(-\frac{(2n-1)^2}{4h_{Di+1}^2}\pi^2\beta\tau\right)\sin\left(\frac{2n-1}{2}\right)\pi\frac{z_{wDi+1}}{h_{Di+1}}\sin\left(\frac{2n-1}{2}\right)\pi\frac{z_{Di+1}}{h_{Di+1}}d\tau \qquad (3.10)$$

3.1.3 No Crossflow Interface

When there is an impermeable interface each layer behaves like an independent reservoir. The layers are commingled in a common (parent) wellbore. Therefore, the dimensionless pressure expressions for the layers are

$$p_{Dj}\left(x_{Dj},y_{Dj},z_{Dj},t_D\right)=\frac{\sqrt{\pi}}{4}\int_0^{t_D}\left[erf\left(\frac{1+x_{Dj}}{2\sqrt{\tau}}\right)\right.$$

$$\left.+erf\left(\frac{1-x_{Dj}}{2\sqrt{\tau}}\right)\right]\frac{e^{-\frac{\left(y_{Dj}-y_{wDj}\right)^2}{4\tau}}}{\sqrt{\tau}}\left[1+\frac{1}{2}\sum_{n=1}^{\infty}\exp\left(-\frac{n^2\pi^2\tau}{4h_{Dj}^2}\right)\cos n\pi\frac{z_{Dj}}{h_{Dj}}\cos n\pi\frac{z_{wDj}}{h_{Dj}}\right]d\tau \qquad (3.11)$$

where j = layer i or $i+1$

4.0 Early Radial Period Pressure Approximations

When no boundary of any kind has been felt, the pressure behaviour is similar to one obtainable in an infinite reservoir. No matter how thin a reservoir may be and no matter how small and short the well radius and length are, this behaviour must be exhibited at the instance a well is opened until the nearest boundary is felt. During this period, the reservoir pressure changes rapidly with time, and

$$p_D=\frac{\alpha h_D}{8}\int_0^{t_D}\frac{e^{-\frac{(z_D-z_{wD})^2+(z_D-z_{wD})^2}{4\tau}}}{\sqrt{\tau}}d\tau \qquad (4.1)$$

which yields the exponential integral solution

$$p_D=\frac{-\alpha h_D}{8}E_i\left(-\frac{R^2}{4t_D}\right) \qquad (4.2)$$

where $\alpha = 2$ if $x_D \prec 1$, 1 if $x_D = 1$, and 0 if $x_D \succ 1 \cdot R^2 = (z_D - z_{wD})^2 + (z_D - z_{wD})^2$

5.0 Early Linear Period Pressure Approximations

5.1. Crossflow

When there is crossflow between thelayers, the entire reservoir will behave as one enlarged reservoir, especially when the entire interface length is permeable. Early linear period pressure distribution is achieved at t_D corresponding to $\left(\frac{1+x_D}{2\sqrt{t_D}}\right)\geq 1.8$. Beyond this time, flow is flourishing in the x-y plane. This, however, occurs at top of the entire reservoir, that is, at $h_D = h_D + h_{Di+1}$.

5.2 No Crossflow

The early linear period occurs for each layer after the top of the layer is felt by flow transients. Here, at this time, the error function is less than unit.

6.0 Computation of Well Responses

All integrations with respect to time were performed numerically according to the suggestions in [8] and [9]. It should be noted that $h_{Dj} \leq z_{Dj} + z_{wDj} \prec h_D$, and that the dimensionless times for start or end of a particular flow period can best estimated from a plot of p_D against log (t_D). Pressure distribution observed shortly after these periods will reveal the actual nature of the reservoir boundaries. To simulate an infinite-conductivity wellbore [12] $x_{Dj} = 0 \cdot 732;\ 0 \leq x_{Dj} \prec 0 \cdot 732$ represent uniform flux wellbore. Fore dimensionless wellbore pressures very small values of wellbore widths, y_{wD} and radii are used because the wells are line sources. $x_D \geq 2$ means full well penetration along the x-direction. When interlayer flow situations are considered, for example, in both secondary and tertiary recovery projects, the actual values of β are calculated for a given set of reservoir and wellbore properties, using equation (2.13). The final dimensionless pressure is obtained by superposition of the dimensionless pressures due to (1) early time behaviour (from $t_D = 0$ to $t_D = \infty$, and (2) any other flow period possible within the flow time of interest.

7.0 Discussion of Results

7.1 Effects of Well stand-off z_{wD} on p_{wD}

Dimensionless wellbore pressure p_{wD} were generated for both crossflow and no-crossflow systems. The results are shown in Tables 1 to 2 respectively. From the results, it is clear that dimensionless wellbore pressures are unaffected by well locations.

7.2 Effects of Wellbore Radius on p_{wD}

To understand the effects of wellbore radius on wellbore pressure, p_{wD} values were computed for r_{wD} values of $5\times10^{-5}, 10^{-4}$ and 5×10^{-4} (in an increasing order) for crossflow layers with different thickness. The wellbore dimensionless length, L_D is the reciprocal of h_D. The well responses are shown in Tables 3 and 4. Using the same thickness well responses were also computed for no crossflow layers. The results for the no crossflow case are shown in Table 5.

From the results in Tables 3 and 5, it is clear in all cases that layer p_{wD} values are obtained with smaller wellbore radius. The differences in p_{wD} values are significant at early times and reduce to less significant values at late times. For example, in Table 5, the differences are about 20% at early times and less than 7% at late times. It is noticed, too, that the thicker the reservoir the larger the dimensionless wllbore pressures. Therefore, based on wellbore half-length, narrow wells offer excellent productivities at early times.

7.3 Effect of Well length on Well Response

To study the effect of length on well responses, well responses for cross flow and no-cross flow were computed for reservoir dimensionless thickness of 0.8, 1.2, 2.0 and 3. These translate to dimensionless well lengths of 1.25, 0.83, 0.5 and 0.33, respectively, for an isotropic reservoir layers. Well stand-off values were 0.2, 0.3, 0.5 and 0.75 for a fixed value of $r_{wD} = 5\times10^{-5}$. The results are shown below in Tables 6a and 6b. As discussed in [5] and [12], and revealed also in Tables 6a and 6b, the longer the wellbore lengths, the lower the productivities for fixed values of z_{wD} and r_{wD}. Long wells produce the effects of pressure transient attenuation; from the point of measurement the wellbore pressure transient decreases as the length of propagation increases. At early times the effects of well length, in both crossflow and no-crossflow systems are exactly the same as no boundary is felt. At long times, however, when different boundaries are encountered, the p_{wD} values increase in equal amounts but those of no-crossflow are larger in magnitude.

8.0 Detection of Layering and Crossflow

To detect crossflow, first plot p_{wD} versus t_D on semi-log paper for crossflow for each layer. If crossflow is established, then make the plot for only crossflow case for each layer. Match each curve with those from observed (well flow pressures against time) plot and calculate the permeability for each layer. Equal permeability values mean absence of layering. Different permeability values mean presence of layering. This approach is discussed and used in [17] and [14].

As shown in Tables 7 and 8, for the layered reservoir with crossflow the p_{wD} values are about the same as those of no crossflow at early times. But at late times the dimensionless wellbore pressures of no crossflow layers appreciate to between approximately 1.02 and 1.12 times those of crossflow. Furthermore, no crossflow systems exhibit earlier departure from early radial behaviour and earlier pseudosteady behaviour than crossflow system.

9.0 Validation of Results

Following he difference in the definition of z_D in our case and those of other authors, [12], [15], [16], a basis for comparison with these model results exist only for $h_D = L_D = 1 \cdot 0$. For this condition, dimensionless wellbore pressures were calculated for some dimensionless wellbore parameters using our models. This basis is, however, necessary only at long times. For early times differences in dimensionless parameters definitions do not affect the results. This is because at early wellbore pressures exhibit infinite reservoir behaviour. For early times, therefore, the calculated results are compared with some other results [12], [15] and [16] as shown in Table 9. The dimensionless pressures show an acceptable closeness between all the authors (including ours).

10.0 Application to Displacement Stability Predictions

The unique set of operational parameters, such as wellbore properties, reservoir layers and fluid properties, which can create a delay or completely prevent breakthrough, is measured using the mobility ratio, M, derived in equation (3.4). The mobility ratio compares the velocities of both the displacing and the displaced fluids, and is usually less than unity (best condition) for any set of wellbore and fluid properties. This flow condition is referred to as favourable or stable displacement. For unfavourable or unstable displacement, M is generally greater than 10. For $M \succ 10$, the displacing fluid travels faster than oil land is produced in large volumes into the producing well. Detailed solutions of equation (3.5) for various wellbore, layers and layers' fluid properties have been discussed in [17] and [18], and are summarized below.

11.0 Effects of Wellbore, layers and layers fluid properties on Displacement Stability

[17] and [18] show that although, water breakthrough times are not strongly sensitive to well spacing, substantial stability can be achieved if the wells are reasonable spaced within the constraint of layers thickness. More stable front is however, achieved when both layers have equal permeability than when the top layer is more permeable. If the reservoir layers have better porosity, the dimensionless breakthrough times for these two cases are appreciable enough for a waterflood in a small and thin reservoir.

Furthermore, an arbitrary increase or decrease in well length does not necessarily lead to achieving stability or instability for the waterflood system. This unpredictable behaviour of well lengths has been found to affect even wellbore pressures in layered reservoirs, [3], [4], [5] and single-layer reservoirs [12]. With a particular set of well lengths appreciable stability could be achieved by ensuring that the well in the less permeable layer is used for injection and the other for production.

The ratios of $\frac{c_{ti}}{c_{ti+1}}$ yield significant stability only when $c_{ti} \succ\succ c_{ti+1}$. This is possible in gas injection and thermal flooding using well i for injection. However, larger $\frac{\mu_i}{\mu_{i+1}}$ ratios yield higher stability. Advantage of these viscosity ratios can be taken in polymer-impregnated waterflooding using well i for injection.

12.0 Conclusions

Mathematical models have been formulated to describe pressure distribution in layered reservoir (with

and without crossflow) containing lateral wells. The studies reveal that

1. For crossflow layers, pressure distribution in the layers approximates that of a single layer with equivalent single layer properties.
2. The effects of wellbore properties, on overall productivity in a layered reservoir, are similar to that of a horizontal or lateral well in a single layer reservoir.
3. Crossflow layers fluid production is more economical in terms of productivity than completing individual layers for production.
4. Crossflow and layering can be detected by observation of pressure gradients and type cure matching.
5. Lateral wells in layered reservoirs can be utilized for better oil recovery,

Nomenclature

c	total compressibility, *1/psi*	x	point along x-axis
E	dimensionless weighting factor for the z-source function	y	point along y-axis
L	wellbore length, *ft*	z	point along z-axis
k	permeability, *md*	ϕ	porosity, *fraction*
h	pay thickness, *ft*	μ	viscosity, *cp*
M	mobility ratio	τ	dummy integration variable
md	millidarcy	**Subscripts**	
p	pressure, *psi*	D	dimensionless
Δ	drop	i	layer i
r	wellbore radius, *ft*	$i+1$	layer $i+1$
t	time, *hours*	j	i *or* $i+1$
s	source function symbol	t	total
		w	wellbore

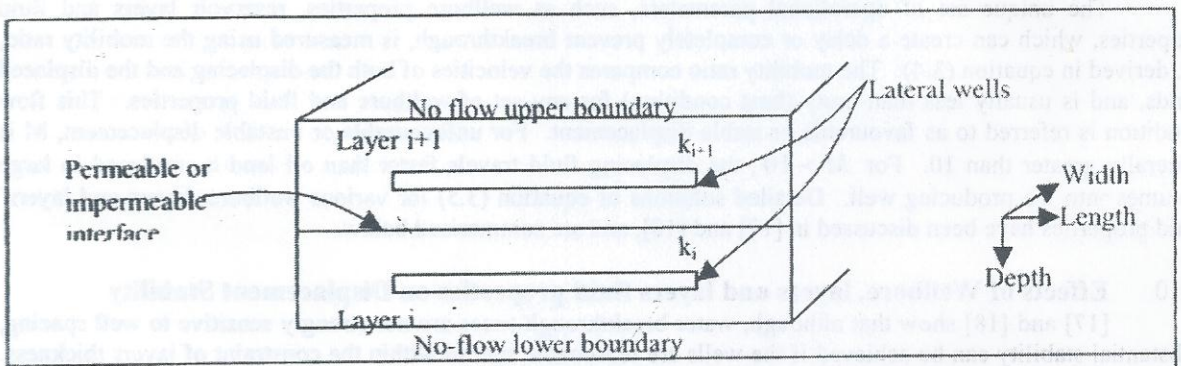

Fig.1: Layered Reservoir Model

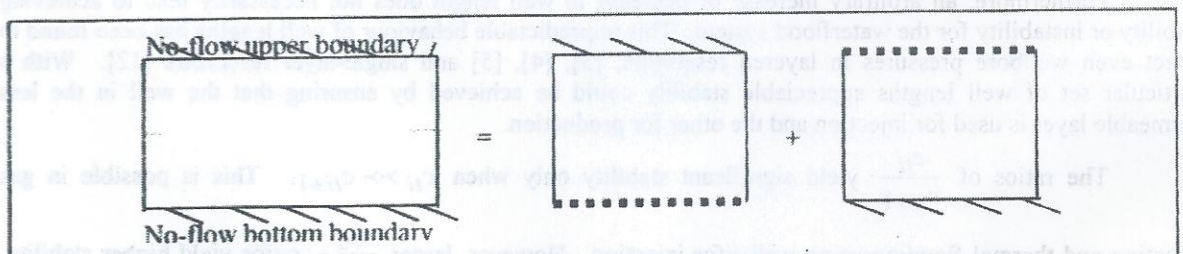

Fig.2: Reservoir Mixed Boundaries on the z-axis.

Table 1: Effects of Wellbore Stand-off on p_{wD}: Cross flow layer i
$h_D = 2, h_{Di} = 1.0 = h_{Di+1}, y_{wDi} = y_{eDi+1} = 1 \times 10^{-4}, x_{Di} = x_{Di+1} = 1.0$

t_D	$z_{wD1} = 0.1$	0.2	0.6	0.8
10^{-6}	1.7001	1.7001	1.7001	1.7001
10^{-5}	2.2758	2.2758	2.2758	2.2758
10^{-4}	2.8514	2.8514	2.8514	2.8514
10^{-3}	3.4271	3.4271	3.4271	3.4271
10^{-2}	4.0027	4.0027	4.0027	4.0027
10^{-1}	4.5784	4.5784	4.5784	4.5784
1	5.1540	5.1540	5.1540	5.1540
10	5.7297	5.7297	5.7297	5.7297

Table 2: Effects of Wellbore Stand off on p_{wD} using well i (not Crossflow)
$h_{Di} = 1.0 = h_{Di+1}, y_{wDi} = y_{wDi+1} = 1 \times 10^{-4}$

t_D	z_{WD1}=0.1	0.2	0.4	0.5
0.000001	2.707	2.707	2.707	2.707
0.00001	3.858	3.858	3.858	3.858
0.0001	5.010	5.010	5.010	5.010
0.001	6.161	6.161	6.161	6.161
0.01	7.312	7.312	7.312	7.312
0.1	8.464	8.464	8.464	8.464
1	9.615	9.615	9.615	9.615
10	10.766	10.766	10.766	10.766
100	11.917	11.917	11.917	11.917

Table 3: Effects of Wellbore raidus on p_{wD} (not Crossflow)
$h_D = 2, z_{wDi} = 0.7, z_{wDi+1} = 0.05, h_{Di} = 1.0, h_{Di-1} = 1.0, \beta = 1 \cdot 0, x_{Di} = 0.732$

t_D	$r_{wDi} = r_{Di+1} = 5 \times 10^{-5}$		10^{-4}		5×10^{-4}	
	Well i	Well i+1	Well i	Well i+1	Well i	Well i+1
10^{-6}	1.7001	1.7001	1.3536	1.3536	0.5486	0.5486
10^{-5}	2.2758	2.2758	1.9292	1.9292	1.1245	1.1245
10^{-4}	2.8514	2.8514	2.5049	2.5049	1.7001	1.7001
10^{-3}	3.4217	3.4217	3.0805	3.0805	2.2758	2.2753
10^{-2}	4.0027	3.8643	3.6562	3.6562	2.8514	2.8514
10^{-1}	4.5784	4.0027	4.2318	3.5177	3.4271	3.3228
1	5.1540	4.4741	4.8075	4.1276	4.0027	4.0045

Table 4: Effects of Wellbore raidus on p_{wD} (Crossflow) assuming one well bore
$h_D = 2,\ x_{Di} = 0.732,\ \beta = 1\cdot 0,\ z_{wDi} = 0.05,$

t_D	$r_{wD} = 5x\ 10^{-5}$	10^{-4}	$5x10^{-4}$
10^{-6}	3.4003	2.7071	1.0977
10^{-5}	4.5516	3.8584	2.2490
10^{-4}	5.7029	5.0097	3.4002
10^{-3}	6.8542	6.1610	4.5516
10^{-2}	8.0055	7.3123	5.7029
10^{-1}	9.1568	8.4636	6.8542
1	10.308	9.6149	8.0055
10	11.4593	10.7662	9.1568

Table 5: Effects of Wellbore raidus on p_{wD} (No Crossflow)
$h_D = L_D = 1\cdot 0,\ x_{Di} = 0.732,\ \beta = 1\cdot 0,$

t_D	$r_{wD} = 5x\ 10^{-5}$	10^{-4}	$5x\ 10^{-4}$
10^{-6}	17001	1.3536	0.5489
10^{-5}	2.2758	1.9292	1.1243
10^{-4}	2.8514	2.5049	1.7001
10^{-3}	3.4271	3.0805	2.2758
10^{-2}	4.1060	3.7594	2.9547
10^{-1}	5.5365	5.1900	4.3853
1	6.4712	6.1246	5.3199

Table 6a: Effects of Well length on p_{wD} (Crossflow) $x_D = 0.732$

L_D	$t_D = 10^{-6}$	10^{-5}	10^{2}	10^{3}
1.25	1.3601	1.8206	5.0443	5.5048
0.83	2.0402	2.7310	7.5664	8.2572
0.50	3.4003	4.5516	12.6106	13.7619
0.33	5.1004	6.8274	18.9160	20.6429

Table 6b: Effects of Well length on p_{wD} (No Crossflow) $x_D = 0.732$

L_D	$t_D = 10^{-6}$	10^{-5}	10^{2}	10^{3}
1.25	1.3602	1.8206	6.8514	7.3350
0.83	2.0402	2.7310	9.3735	10.0874
0.50	3.4003	4.5516	14.4177	15.5921
0.33	5.1004	6.8274	20.7231	22.4731

Table 7: Dimensionless Wellbore Pressure (Infinite Conductivity) Crossflow (Layer *i*)

h_{Di+1} = h_D-h_{Di}, y_{WDi} =y_{wdi+1}=5x10^{-5}				
h_D =	0.8	1.2	2.0	3.0
h_{Di} =	0.4	0.6	1.0	1.5
z_{wDi} =	0.2	0.3	0.5	0.75
z_{Di+1} =	0.2	0.3	0.5	0.75
z_{Di} =	0.2	0.3	0.5	0.75
z_{wDi+1} =	0.2	0.3	0.5	0.75
Dimensionless Time,t_D				
0.000001	1.3601	2.0402	3.4003	5.1004
0.00001	1.8206	2.7310	4.5516	6.8274
0.0001	2.2812	3.4217	5.7029	8.5543
0.001	2.7417	4.1125	6.8542	10.2813
0.01	3.2022	4.8033	8.0055	12.0082
0.1	3.6627	5.4941	9.1568	13.7351
1	4.1232	6.1848	10.3081	15.4621
10	4.5837	6.8756	11.4593	17.1890

Table 8: Dimensionless Wellbore Pressure (Infinite Conductivity) No Crossflow (Layer *i*)

h_{Di+1} = h_D-h_{Di}, y_{WDi} =y_{WDi+1}=5x10^{-5}				
h_D =	0.8	1.2	2.0	3.0
h_{Di} =	0.4	0.6	1.0	1.5
z_{wDi} =	0.2	0.3	0.5	0.75
z_{Di+1} =	0.2	0.3	0.5	0.75
z_{Di} =	0.2	0.3	0.5	0.75
z_{wDi+1} =	0.2	0.3	0.5	0.75
Dimensionless Time,t_D				
0.000001	1.3602	2.0402	3.4003	5.1004
0.00001	1.8206	2.7310	4.5516	6.8274
0.0001	2.2812	3.4217	5.7029	8.5543
0.001	2.7417	4.1125	6.8542	10.2813
0.01	3.2746	4.8606	8.0407	12.0782
0.1	4.1987	6.0143	9.5458	14.499
1	5.0798	7.1601	11.2569	16.7754
10	6.1954	8.4873	13.0710	18.897

Table 9: Comparison of results of some authors for Dimensionless Wellbore Pressure
$x_D = 0.732,\ y_D = 0 \cdot 0005,\ h_D = 1 \cdot 0$ (No Crossflow)

t_D	Ref.14.	Ref.10.	Ref.15.	Our results
0.000001	0.05490	0.05472	0.05507	0.05489
0.00001	0.1124	0.1126	0.11245	0.11245
0.0001	0.17007	0.1700	0.11260	0.17001
0.001	0.22888	0.2288	0.17098	0.22758
0.01	0.34958	0.3495	0.29164	0.29547
0.1	0.66767	0.6675	0.60972	0.66853
1	1.37630	1.3760	1.31828	1.34005

References

[1] Russell, D. G. and Prats, M. (1962) Perfomance of Layered Reservoirs with Crossflow – Single Compressible-Fluid Case, Trans., AIME, 225, 53 – 67.

[2] Katz. L. M. and Tek, M. R. (1962) A Theoretical Study of Pressure Distribution and Fluid Flux in Bounded Stratified Porous System with Crossflow. Trans., AIME, 255, 68 – 82.

[3] Kuchuck, F. J. (1991) Pressure Derivative of Horizontal Wells in Multi-Layer Reservoirs with Crossflow, SEP 22731 presented at the SPE Annual Technical Conference and Exhibition, Dallas.

[4] Suzuki, K. and Namba, T (1991) Horizontal Well Pressure Transient Behaviour in Stratified Reservoirs, SPE 22732 presented at the SPE Annual Technical Conference and Exhibition, Dallas.

[5] Adewole, E. S., Rai, B. M. and Audu, T. O. K. (2000) Effects of Oil Well Length on Pressure Drawdown in Layered Reservoirs, J. Nigeria Ass. of Mathematical Physics, 4, 259

[6] Adewole, E. S., Rai, B. M. and Audu, T. O. K. (2002) Interference Test Analysis of Pressure Data from Lateral Wells in a Layered Reservoir with Crossflow, paper JSTR-2002-069 accepted for publication in the J. of Science and Technology Research.

[7] Gringarten, A. C. and Ramey, H. J. (Jr) (1973) The Use of Source and Green's Functions in Volving Unsteady-Flow Problems in Reservoirs, SPE Trans., AIME, 1973, 255 – 285.

[8] Carslaw, H. S. and Jaeger, J. C. (1959) Conduction of Heat through Solids. London, England 2nd Ed.., Oxford U. Press.

[9] Adewole, E. S., Rai, B. M. and Audu, T. O. K. (2002) Mathematical Models of Selected Reservoir Systems involving Horizontal Wells, paper JSTR-2002-081 Accepted for Publication in the J. of Science and Technology, University of Uyo.

[10] Adewole, E. S., Rai, B. M. and Audu, T. O. K. (2001) The use of Gauss-Legendre Quadrature in Solving Flow Problems in Horizontal Wells, J. Nigeria Ass. of Mathematical Physics, 5, 89.

[11] Suzuki, K. and Namba, T. (1990) Horizontal Well Test Analysis System, paper SPE 20613 prepared for presentation at the 65th Annual Technical Conference and Exhibition of the Society of Petroleum

[12] Ozkan, E. and Raghavan, R. (1990) Performance of Horizontal Wells Subject to Bottom Water Drive, SPERE, Trans., AIME, 289, 375 – 383.

[13] Falade, G. K. (1980) Application of Type Curves Analysis in Interpreting Pressure Data from a Stratified Reservoir, Jo\. of Canadian Petroleum Technology, 74 - 79

[14] Agarwal, R. G., Al-Hussainy, R. and Ramey, H. J. Jr. (1970) An Investigation of Wellbore Storage and Skin Effects in Unsteady Liquid Flow: I. Analytical Treatment SPEJ Trans; AIME, 249, 279 – 90.

[15] Clonts, M. D. and Ramey, J. J. (Jr.) (1986) Pressure-Transient Analysis for Wells Horizontal Drainholes, Paper SPE 15116 presented at the 1986 SPE California Regional Meeting, Oakland.

[16] Malekzadeth, D. and Tiab, D. (1991) Interference Testing of Horizontal Wells, paper SPE 22793 presented at the Annual Technical Conference and Exhibition of SPE held in Dallas, TX.

[17] Adewole, E.S., Rai, B. M. and Audu, T. O. K. (2002) Investigating Stability Criteria for Waterflood Projects using a Layered Reservoir with Lateral Wells, Paper submitted to the Journal of Civil and Environmental Systems Engineering, University of Benin.

[18] Adewole, E. S. (2002) Generalized Stability Criteria for Waterflood Projects using Lateral Wells, Paper submitted to the Journal of Nigerian Institute of Production Engineers, University of Benin.